

Twin Photon Correlations in Single-Photon Interference

Mayukh Lahiri,^{1,*} Armin Hochrainer,¹ Radek Lapkiewicz,² Gabriela Barreto Lemos,^{1,3} and Anton Zeilinger^{1,3}

¹*Vienna Center for Quantum Science and Technology (VCQ), Faculty of Physics, University of Vienna, Boltzmannngasse 5, Vienna A-1090, Austria.*

²*Faculty of Physics, University of Warsaw, Pasteura 5, 02-093 Warsaw, Poland.*

³*Institute for Quantum Optics and Quantum Information, Austrian Academy of Sciences, Boltzmannngasse 3, Vienna A-1090, Austria.*

We show that it is possible to generate a novel single-photon fringe pattern by using two spatially separated identical bi-photon sources. The fringes are similar to the ones observed in a Michelson interferometer and possess certain remarkable properties with potential applications. A striking feature of the fringes is that although the pattern is obtained by detecting only one photon of each photon pair, the fringes shift due to a change in the optical path traversed by the undetected photon. The fringe shift is characterized by a combination of wavelengths of both photons, which implies that the wavelength of a photon can be measured without detecting it. Furthermore, the visibility of the fringes diminishes as the correlation between the transverse momenta of twin photons decreases: visibility is unity for maximum momentum correlation and zero for no momentum correlation. We also show that the momentum correlation between the two photons of a pair can be determined from the single-photon interference pattern. We thus for the first time propose a method of measuring a two-photon correlation without coincidence or heralded detection.

I. INTRODUCTION

The discovery of the Michelson interferometer [1] is one of the most important events in the history of physics: apart from its relevance to the special theory of relativity [2, 3], it has also been applied in matter-wave interferometry [4], and, most recently, in the detection of gravitational waves [5]. Here we establish that a novel type of single-photon fringe pattern can be created, which looks similar to the one observed in a Michelson interferometer, but possesses some remarkable properties. We produce the fringes using the method of “induced coherence without induced emission” [6, 7]. The method is based on the following quantum mechanical principle: quantum interference occurs if and only if the information regarding the path traversed by a quantum entity is unavailable [8]. This method has already been applied to the areas of imaging [9, 10], spectroscopy [11, 12], optical polarization [13], tests of the complementarity principle [14–17], and microwave superconducting cavities [18].

In a Michelson interferometer, the two interfering beams are produced from an original beam by the method of division of amplitude and the fringe shift associated with a change in optical path is characterized by the wavelength of the interfering beams ([19], Sec. 7.5.4). By contrast, the interfering beams in our case are produced by two spatially separated identical sources each of which generates photon pairs; the fringe shift associated with a change in the optical path is characterized by the wavelengths of both photons that constitutes a pair. This fact can be used to determine the wavelength of a photon without detecting that photon. Furthermore, the visibility of these fringes depends on the correlation

between the transverse momenta of the two photons; in certain cases, this fact allows us to quantitatively determine the momentum correlation between the two photons belonging to a photon pair by detecting only one of the photons.

In Sec. II, we give a summary of the notations to be used in this paper. In Sec. III, we present the main theoretical analysis and discuss the properties of the fringes in detail. Then in Sec. IV, we show that under certain reasonable assumptions it is possible to obtain a measure of the momentum correlation between twin photons from the visibility of the fringe pattern. After that, in Sec. V, we briefly compare the theoretical predictions with experimental observations. Finally, in Sec. VI, we summarize our results and discuss their implications.

II. NOTATIONS

We assume that the two photons, a and b , constituting a pair have, in general, different values of mean frequency (energy). If the associated optical fields are distributed over several plane-wave modes (spatial modes), the quantum state of the photon pair can be represented in the form [21]

$$|\psi\rangle = \sum_{\mathbf{k}_a, \mathbf{k}_b} C_{\mathbf{k}_a, \mathbf{k}_b} |\mathbf{k}_a\rangle_a |\mathbf{k}_b\rangle_b, \quad (1)$$

where $|\mathbf{k}_a\rangle_a$ denotes a single a -photon occupation in the mode labeled by the wave vector \mathbf{k}_a and the complex amplitudes $C_{\mathbf{k}_a, \mathbf{k}_b}$ assure that the state $|\psi\rangle$ is normalized.

The joint probability (density) of photon a having momentum $\mathbf{p}_a = \hbar\mathbf{k}_a$ and photon b having momentum $\mathbf{p}_b = \hbar\mathbf{k}_b$ is equal to

$$P(\mathbf{k}_a, \mathbf{k}_b) = |C_{\mathbf{k}_a, \mathbf{k}_b}|^2. \quad (2)$$

*Electronic address: mayukh.lahiri@univie.ac.at

The conditional probability of photon a to have momentum $\hbar\mathbf{k}_a$ given photon b carries momentum $\hbar\mathbf{k}_b$ is given by

$$\mathcal{P}(\mathbf{k}_a|\mathbf{k}_b) \equiv \frac{P(\mathbf{k}_a, \mathbf{k}_b)}{P(\mathbf{k}_b)} = \frac{|C_{\mathbf{k}_a, \mathbf{k}_b}|^2}{\sum_{\mathbf{k}_a} |C_{\mathbf{k}_a, \mathbf{k}_b}|^2}, \quad (3)$$

where $P(\mathbf{k}_b) = \sum_{\mathbf{k}_a} P(\mathbf{k}_a, \mathbf{k}_b) = \sum_{\mathbf{k}_a} |C_{\mathbf{k}_a, \mathbf{k}_b}|^2$ is the probability of photon b having momentum $\hbar\mathbf{k}_b$. Similarly, $\mathcal{P}(\mathbf{k}_b|\mathbf{k}_a) = |C_{\mathbf{k}_a, \mathbf{k}_b}|^2/P(\mathbf{k}_a)$ and $P(\mathbf{k}_a) = \sum_{\mathbf{k}_b} |C_{\mathbf{k}_a, \mathbf{k}_b}|^2$.

The correlation between \mathbf{p}_a and \mathbf{p}_b is governed by $P(\mathbf{k}_a, \mathbf{k}_b)$. For example, when \mathbf{p}_a and \mathbf{p}_b are fully uncorrelated (statistically independent), the conditional probability $\mathcal{P}(\mathbf{k}_a|\mathbf{k}_b) = P(\mathbf{k}_a)$; in this case the joint probability takes the form $P(\mathbf{k}_a, \mathbf{k}_b) = P(\mathbf{k}_a)P(\mathbf{k}_b)$. It is thus clear from Eq. (1) that if the quantum state can be expressed in the product form $|\psi\rangle = |\psi_a\rangle \otimes |\psi_b\rangle$, the momenta of the photons are uncorrelated.

Throughout this paper we assume that the photons propagate as paraxial beams and are incident normally on a detector. Therefore, the correlation between momenta is to be understood as correlation between *transverse* momenta of the photons.

III. SINGLE-PHOTON INTERFERENCE USING TWO IDENTICAL BIPHOTON SOURCES

Let Q_1 and Q_2 be *identical* sources (Fig. 1), each of which generates biphoton states given by Eq. (1). Source Q_j ($j = 1, 2$) emits photons a and b into the beams a_j and b_j , respectively. The beams, b_1 and b_2 , are superposed by a beam splitter, BS. They interfere if and only if one cannot identify the path (b_1 or b_2) traversed by photon b that emerges from an output of BS. No path information is available if one takes the two following measures [7, 20]: 1) choosing the optical path lengths appropriately; 2) sending beam a_1 through Q_2 and aligning it with beam a_2 such that the spatial modes present in a_2 are identical with those present in a_1 . We assume that the simultaneous presence of photons generated by both sources is highly improbable; this also implies that almost no stimulated emission occurs at Q_2 . Under these circumstances the quantum state of light in the system is given by (see Appendix 1; cf. [6, 7, 10])

$$|\Psi\rangle = \alpha_1 \sum_{\mathbf{k}_{a_1}, \mathbf{k}_{b_1}} C_{\mathbf{k}_{a_1}, \mathbf{k}_{b_1}} |\mathbf{k}_{a_1}\rangle_{a_1} |\mathbf{k}_{b_1}\rangle_{b_1} + \alpha_2 \sum_{\mathbf{k}_{a_2}, \mathbf{k}_{b_2}} \exp[-i\phi_a(\mathbf{k}_a)] C_{\mathbf{k}_{a_2}, \mathbf{k}_{b_2}} |\mathbf{k}_{a_2}\rangle_{a_1} |\mathbf{k}_{b_2}\rangle_{b_2}, \quad (4)$$

where $\phi_a(\mathbf{k}_a)$ is the phase acquired by the plane-wave mode \mathbf{k}_a due to propagation from Q_1 to Q_2 , α_1 and α_2 are complex numbers obeying $|\alpha_1|^2 + |\alpha_2|^2 = 1$; $|\alpha_j|$ characterizes the rate of emission from Q_j .

One of the outputs of BS is focused by a thin positive lens, L0, on a camera, C. Within the diffraction limit, the positive lens maps a plane wave with wave vector

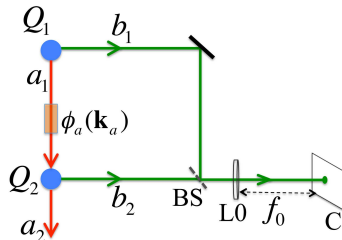


FIG. 1: Schematic of the proposed experiment. Biphoton sources Q_j emit photons a and b into beams a_j and b_j . Beam a_1 is sent through Q_2 and aligned with a_2 . The b -photon beams generated by the sources are superposed by a beam splitter, BS, and one of the outputs of BS is focused by a positive lens, L0, of focal length f_0 on a camera, C. A plane-wave (\mathbf{k}_a) mode of photon a gains phase $\phi_a(\mathbf{k}_a)$ due to propagation from Q_1 to Q_2 .

\mathbf{k}_b on a point, $\boldsymbol{\rho}_{\mathbf{k}_b}$, on the camera (Fig. 2). The positive frequency part of the quantized field at $\boldsymbol{\rho}_{\mathbf{k}_b}$ can, therefore, be expressed as (see also, [10])

$$\hat{E}_b^{(+)}(\boldsymbol{\rho}_{\mathbf{k}_b}) = \hat{a}_{b_1}(\mathbf{k}_b) + i \exp[i\phi_b(\mathbf{k}_b)] \hat{a}_{b_2}(\mathbf{k}_b), \quad (5)$$

where $\hat{a}_{b_j}(\mathbf{k}_b)$ is the photon-annihilation operator such that $\hat{a}_{b_j}^\dagger(\mathbf{k}_b) \hat{a}_{b_j}(\mathbf{k}_b) |\mathbf{k}_b\rangle_{b_j} = \delta_{jl} |\mathbf{k}_b\rangle_{b_j}$, and $\phi_b = \phi_{b_2} - \phi_{b_1}$ is the phase difference resulting from different propagation lengths of the beams b_1 and b_2 . Apart from a pro-

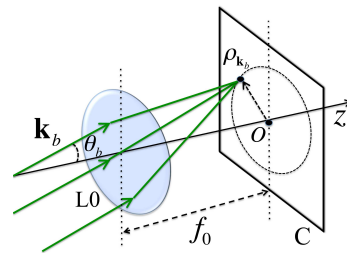


FIG. 2: Detection system geometry. L0 is a positive lens with focal length f_0 . The origin (O) is chosen at the point where the optical axis (beam axis) z meets the detection plane (camera). The wave vector \mathbf{k}_b makes an angle θ_b with the optical axis. Plane waves making an angle θ_b with the z axis are focused along a circle of radius $|\boldsymbol{\rho}_{\mathbf{k}_b}| \approx f_0 \theta_b$ centered at O ; $\boldsymbol{\rho}_{\mathbf{k}_b}$ is a two-dimensional position vector.

portionality constant, the photon counting rate [22] at a point in the camera is given by

$$\mathcal{R}(\boldsymbol{\rho}_{\mathbf{k}_b}) \equiv \langle \Psi | \hat{E}_b^{(-)}(\boldsymbol{\rho}_{\mathbf{k}_b}) \hat{E}_b^{(+)}(\boldsymbol{\rho}_{\mathbf{k}_b}) | \Psi \rangle, \quad (6)$$

where $\hat{E}_b^{(-)}(\boldsymbol{\rho}_{\mathbf{k}_b}) = \{\hat{E}_b^{(+)}(\boldsymbol{\rho}_{\mathbf{k}_b})\}^\dagger$. It follows from Eqs. (4), (5), and (6) that

$$\mathcal{R}(\boldsymbol{\rho}_{\mathbf{k}_b}) = \sum_{\mathbf{k}_a} |C_{\mathbf{k}_a, \mathbf{k}_b}|^2 \{ |\alpha_1|^2 + |\alpha_2|^2 + 2|\alpha_1||\alpha_2| \cos[\phi_b(\mathbf{k}_b) - \phi_a(\mathbf{k}_a) + \phi_2 - \phi_1] \}, \quad (7)$$

where $\phi_1 = \arg\{\alpha_1\}$, $\phi_2 = \arg\{\alpha_2\}$, \arg being the argument of a complex number. Clearly, phase changes introduced by both a - and b -photons modulate the photon counting rate.

We are interested in the case where the photon counting rate at the camera is modulated only by the phase term, $\phi_a(\mathbf{k}_a)$, i.e., by the phase introduced by photon a ; we assume that $\phi_a(\mathbf{k}_a)$ is *not* a slowly varying function of \mathbf{k}_a . We set the difference between the optical path traversed by b_1 and b_2 small enough such that $\phi_b(\mathbf{k}_b)$ becomes a slowly varying function of \mathbf{k}_b and can be treated as a constant. If we also assume that the sources emit at the same rate (i.e., $|\alpha_1| = |\alpha_2|$), Eq. (7) reduces to the form

$$\mathcal{R}(\boldsymbol{\rho}_{\mathbf{k}_b}) \propto \sum_{\mathbf{k}_a} |C_{\mathbf{k}_a, \mathbf{k}_b}|^2 \{1 + \cos[\phi_a(\mathbf{k}_a) - \phi_0]\}, \quad (8)$$

where all other phase terms are included in ϕ_0 . Note that the cosine term cannot be pulled out of the summation, which suggests that several spatial modes (\mathbf{k}_a) of an a -photon can contribute to the photon counting rate at a single point ($\boldsymbol{\rho}_{\mathbf{k}_b}$) on the camera. Furthermore, these contributions are weighted with the joint probability $\mathcal{P}(\mathbf{k}_a, \mathbf{k}_b) = |C_{\mathbf{k}_a, \mathbf{k}_b}|^2$. The correlation between the transverse momenta of photons a and b thus affects the properties of the resulting fringe pattern observed on the camera.

In particular, we are interested in the visibility of the fringe pattern. The visibility at a point ($\boldsymbol{\rho}_{\mathbf{k}_b}$) on the fringe pattern is defined by the usual formula [19]

$$\mathcal{V}(\boldsymbol{\rho}_{\mathbf{k}_b}) = \frac{\mathcal{R}_{\max}(\boldsymbol{\rho}_{\mathbf{k}_b}) - \mathcal{R}_{\min}(\boldsymbol{\rho}_{\mathbf{k}_b})}{\mathcal{R}_{\max}(\boldsymbol{\rho}_{\mathbf{k}_b}) + \mathcal{R}_{\min}(\boldsymbol{\rho}_{\mathbf{k}_b})}, \quad (9)$$

where $\mathcal{R}_{\max}(\boldsymbol{\rho}_{\mathbf{k}_b})$ and $\mathcal{R}_{\min}(\boldsymbol{\rho}_{\mathbf{k}_b})$ are maximum and minimum values of the photon counting rate, respectively, at the point $\boldsymbol{\rho}_{\mathbf{k}_b}$; the maximum and minimum values are obtained by varying the phase term ϕ_0 .

In the subsections below, we discuss the relationship between the fringe visibility and momentum correlation between photons a and b . We consider three cases where the momenta are maximally, minimally, and partially correlated.

A. Maximal Momentum Correlation

Suppose that photons a and b have mean frequencies $\bar{\omega}_a$ and $\bar{\omega}_b$, respectively, such that the moduli of the associated wave vectors in the vacuum are given by $|\mathbf{k}_a| = \bar{\omega}_a/c$ and $|\mathbf{k}_b| = \bar{\omega}_b/c$, c being the speed of light in vacuum. We further assume that the beam axis is identical with the optical axis, i.e., the symmetry axis of the optical system.

We first consider the situation in which the momenta of photons a and b are maximally correlated, i.e., if photon b is detected in mode \mathbf{k}_b , photon a must be detected in mode $\mathbf{k}_a = \mathbf{f}(\mathbf{k}_b)$, where the vector $\mathbf{f}(\mathbf{k}_b)$ is uniquely

defined for any \mathbf{k}_b . One thus has $\mathcal{P}(\mathbf{k}_a|\mathbf{k}_b) = \delta_{\mathbf{k}_a, \mathbf{f}(\mathbf{k}_b)}^{(3)}$, where $\delta_{\mathbf{k}, \mathbf{k}'}^{(3)} = 1$ for $\mathbf{k} = \mathbf{k}'$, and $\delta_{\mathbf{k}, \mathbf{k}'}^{(3)} = 0$ for $\mathbf{k} \neq \mathbf{k}'$; i.e.,

$$|C_{\mathbf{k}_a, \mathbf{k}_b}|^2 = P(\mathbf{k}_b) \delta_{\mathbf{k}_a, \mathbf{f}(\mathbf{k}_b)}^{(3)}. \quad (10)$$

It now follows from Eqs. (8) and (10) that

$$\mathcal{R}(\boldsymbol{\rho}_{\mathbf{k}_b}) \propto P(\mathbf{k}_b) \{1 + \cos(\phi_a[\mathbf{k}_a = \mathbf{f}(\mathbf{k}_b)] - \phi_0)\}. \quad (11)$$

Let d_a be the effective propagation distance between Q_1 and Q_2 along the axis of the beam a_1 . The length of the optical path traveled along \mathbf{k}_a that forms an angle θ_a with the beam axis, is given by $n(\bar{\omega}_a)d_a/\cos\theta_a$; one therefore has

$$\phi_a(\mathbf{k}_a) = \frac{\bar{\omega}_a}{c} \frac{n(\bar{\omega}_a)d_a}{\cos\theta_a} \approx \frac{\bar{\omega}_a}{c} n(\bar{\omega}_a)d_a \left(1 + \frac{\theta_a^2}{2}\right), \quad (12)$$

where $n(\bar{\omega}_a)$ is the refractive index of the medium between Q_1 and Q_2 . By choosing an appropriate value of ϕ_0 , it is possible to set $\bar{\omega}_a n(\bar{\omega}_a)d_a/c - \phi_0$ equal to a multiple of 2π . Equation (11) now becomes

$$\mathcal{R}(\boldsymbol{\rho}_{\mathbf{k}_b}) \propto P(\mathbf{k}_b) \{1 + \cos[\bar{\omega}_a n(\bar{\omega}_a)d_a \theta_a^2 / (2c)]\}. \quad (13)$$

It is clear that when d_a is large enough, interference fringes of unit visibility appear on the camera [23]. The shape of these fringes depends on the relationship between θ_a and $\boldsymbol{\rho}_{\mathbf{k}_b}$, i.e., on the form of $\mathbf{f}(\mathbf{k}_b)$.

To illustrate the phenomenon we assume that photons a and b are emitted into collinear or near-collinear beams and $\mathbf{f}(\mathbf{k}_b) = \mathbf{k}_0 - \mathbf{k}_b$, where \mathbf{k}_0 is a constant vector along the common axis of the beams of a - and b -photons (Fig. 3). It now readily follows that $|\mathbf{k}_a| \sin\theta_a = |\mathbf{k}_b| \sin\theta_b$,

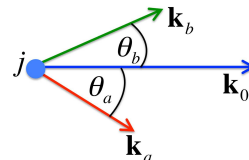


FIG. 3: Illustrating the case $\mathbf{k}_a = \mathbf{f}(\mathbf{k}_b) \approx \mathbf{k}_0 - \mathbf{k}_b$. The constant vector \mathbf{k}_0 is along the common axis of a - and b -photon beams. The angle between \mathbf{k}_a and \mathbf{k}_0 is θ_a ; the angle between \mathbf{k}_b and \mathbf{k}_0 is θ_b . Both θ_a and θ_b are small angles.

where θ_a and θ_b are the angles made by \mathbf{k}_a and \mathbf{k}_b , respectively, with \mathbf{k}_0 [24]. In the small angle limit we then have $\bar{\omega}_a \theta_a \approx \bar{\omega}_b \theta_b$. Since $|\boldsymbol{\rho}_{\mathbf{k}_b}| = f_0 \tan\theta_b \approx f_0 \theta_b$, we obtain the relation $\theta_a \approx \bar{\omega}_b |\boldsymbol{\rho}_{\mathbf{k}_b}| / (f_0 \bar{\omega}_a)$, where f_0 is the focal length of L0 (Fig. 2). Equation (13) now reduces to the form

$$\mathcal{R}(\boldsymbol{\rho}_{\mathbf{k}_b}) \propto P(\mathbf{k}_b) \left\{1 + \cos\left[\frac{\bar{\omega}_b^2}{\bar{\omega}_a} \frac{n(\bar{\omega}_a)d_a}{2cf_0^2} |\boldsymbol{\rho}_{\mathbf{k}_b}|^2\right]\right\}. \quad (14)$$

If $P(\mathbf{k}_b)$ only depends on θ_b , the circular symmetry of Eq. (14) suggests that the fringes are circular in

shape and the minimum value of the photon counting rate across the fringe pattern is zero. Figures 4(a) and 4(b) show the computationally obtained fringe pattern for the following choices of expressions and parameters: $P(\mathbf{k}_b) = \exp[-2\theta_b^2/\sigma_b^2] = \exp[-2\rho_{k_b}^2/(f_0\sigma_b)^2]$, where $\sigma_b = 2.36 \times 10^{-2}$ and $f_0 = 15$ cm; we choose $n(\bar{\omega}_a) = 1$, $\bar{\lambda}_a = 1550$ nm and $\bar{\lambda}_b = 810$ nm.

Equation (14) implies that the condition of a maximum is given by

$$\frac{\bar{\omega}_b^2}{\bar{\omega}_a} \frac{n(\bar{\omega}_a)d_a}{2cf_0^2} (\rho_N)^2 = 2N\pi, \quad N = 0, 1, 2, \dots, \quad (15)$$

where ρ_N is the radius of the N -th bright ring and $N = 0$ characterizes the central maximum. If the medium between Q_1 and Q_2 is nondispersive, it immediately follows that

$$\rho_N \propto \sqrt{N} (\bar{\lambda}_b^2/\bar{\lambda}_a)^{1/2} = \sqrt{N} \bar{\lambda}_{eq}^{1/2}, \quad (16)$$

where $\bar{\lambda}_a$ and $\bar{\lambda}_b$ are mean wavelengths of a and b photons, respectively, and $\bar{\lambda}_{eq} = \bar{\lambda}_b^2/\bar{\lambda}_a$. Clearly, the radius of the N th bright ring is proportional to \sqrt{N} just like the fringes of equal inclination produced in a Michelson interferometer ([19], Sec. 7.5.4). However, in contrast to the Michelson interferometer the fringe shift associated with a change in d_a is *not* characterized by the wavelength of the interfering light but by an equivalent wavelength $\bar{\lambda}_{eq} = \bar{\lambda}_b^2/\bar{\lambda}_a$. We illustrate this fact in Fig. 4(c) by plotting the square of the radius $[(\rho_1)^2]$ of the first ($N = 1$) bright ring (maximum) against the wavelength of the interfering light (λ_b) and comparing it with the case of a traditional Michelson interferometer.

It is possible to determine the wavelength $\bar{\lambda}_{eq}$ from the fringe shift associated with change in d_a . The value of $\bar{\lambda}_a$ can then be obtained if the value of $\bar{\lambda}_b$ is known. Note that photon a is not detected; the fringe pattern is obtained by detecting photon b only. *This implies that one can determine the mean wavelength of photon a without detecting it.*

Equation (11) shows that *the visibility of the fringes is equal to unity for perfect momentum correlation*. Although a perfect correlation can be achieved only in an idealized situation, photon pairs highly correlated in momenta are now regularly generated in laboratories.

B. No Momentum Correlation

We now consider the case in which the momenta of the twin-photons generated by each source are not correlated. As already mentioned in Sec. II, one now has

$$|C_{\mathbf{k}_a, \mathbf{k}_b}|^2 = P(\mathbf{k}_a)P(\mathbf{k}_b). \quad (17)$$

Equation (8) now reduces to

$$\begin{aligned} \mathcal{R}(\rho_{\mathbf{k}_b}) &\propto P(\mathbf{k}_b) \sum_{\mathbf{k}_a} P(\mathbf{k}_a) (1 + \cos[\phi_a(\mathbf{k}_a) - \phi_0]) \\ &= P(\mathbf{k}_b) \times \text{constant}. \end{aligned} \quad (18)$$

In this case, contributions from all \mathbf{k}_a modes get fully averaged out. It is, therefore, clear that a modulation of $\phi_a(\mathbf{k}_a)$ does not result in the creation of interference fringes. We thus conclude that when the momenta of photons a and b are uncorrelated, the visibility of fringes is zero.

C. Partial Momentum Correlation

If the transverse momenta of the photons of a pair are partially correlated, $|C_{\mathbf{k}_a, \mathbf{k}_b}|^2$ can neither be expressed as in Eq. (10) nor as in Eq. (17). As a consequence, the photon counting rate in the camera [Eq. (8)] can no longer be reduced to a simple form. However, we can draw some general conclusions. In this case, the minimum value of intensity at any point of the fringe pattern can never be zero. The visibility of the fringes must, therefore, be less than unity. Furthermore, the number of terms contributing to the sum in Eq. (8) increases with the range over which \mathbf{k}_a varies for a given \mathbf{k}_b . It thus also follows that the larger this range, the lower the visibility of the fringes.

To illustrate the phenomenon let us assume that $\mathcal{P}(\mathbf{k}_a|\mathbf{k}_b)$ is a function of $\mathbf{k}_a + \mathbf{k}_b \equiv \mathbf{k}'$. We write $\mathcal{P}(\mathbf{k}_a|\mathbf{k}_b) \equiv |\mu(\mathbf{k}')|^2$ such that

$$|C_{\mathbf{k}_a, \mathbf{k}_b}|^2 = P(\mathbf{k}_b)|\mu(\mathbf{k}')|^2. \quad (19)$$

It now follows from Eq. (8) that

$$\begin{aligned} \mathcal{R}(\rho_{\mathbf{k}_b}) &\propto P(\mathbf{k}_b) \sum_{\mathbf{k}'} |\mu(\mathbf{k}')|^2 \{1 + \cos[\phi_a(\mathbf{k}' - \mathbf{k}_b) - \phi_0]\}. \end{aligned} \quad (20)$$

We choose $P(\mathbf{k}_b)$ to be given by the same expression as above [see the text below Eq. (14)]. The photon counting rate, $\mathcal{R}(\rho_{\mathbf{k}_b})$, is determined by replacing the summation in Eq. (20) by an integration (see Appendix 2) and assuming

$$\mathcal{P}(\mathbf{k}_a|\mathbf{k}_b) \equiv |\mu(\mathbf{k}')|^2 = \delta(k' - k'_0) \exp[-2\theta'^2/\sigma_\theta^2], \quad (21)$$

where $k' = |\mathbf{k}'|$, k'_0 is a positive constant [25], δ represents the Dirac delta function, θ' is the angle made by \mathbf{k}' with the optical axis, and the positive quantity σ_θ shows how strongly the momenta are correlated [26]: the higher the value of σ_θ , the weaker the correlation between momenta. Figures 4(d) and 4(e) illustrate the computationally obtained fringe pattern for $\sigma_\theta = 9.37 \times 10^{-4}$. A comparison between Figs. 4(a) and 4(d) [or between Figs. 4(b) and 4(e)] shows that the visibility of the fringes is reduced when the momenta of photons a and b are less correlated.

We further investigate the relationship between the visibility of fringes and the momentum correlation by determining the visibility at each point on the fringe pattern. Note that ϕ_0 is independent of \mathbf{k}_a and can be changed

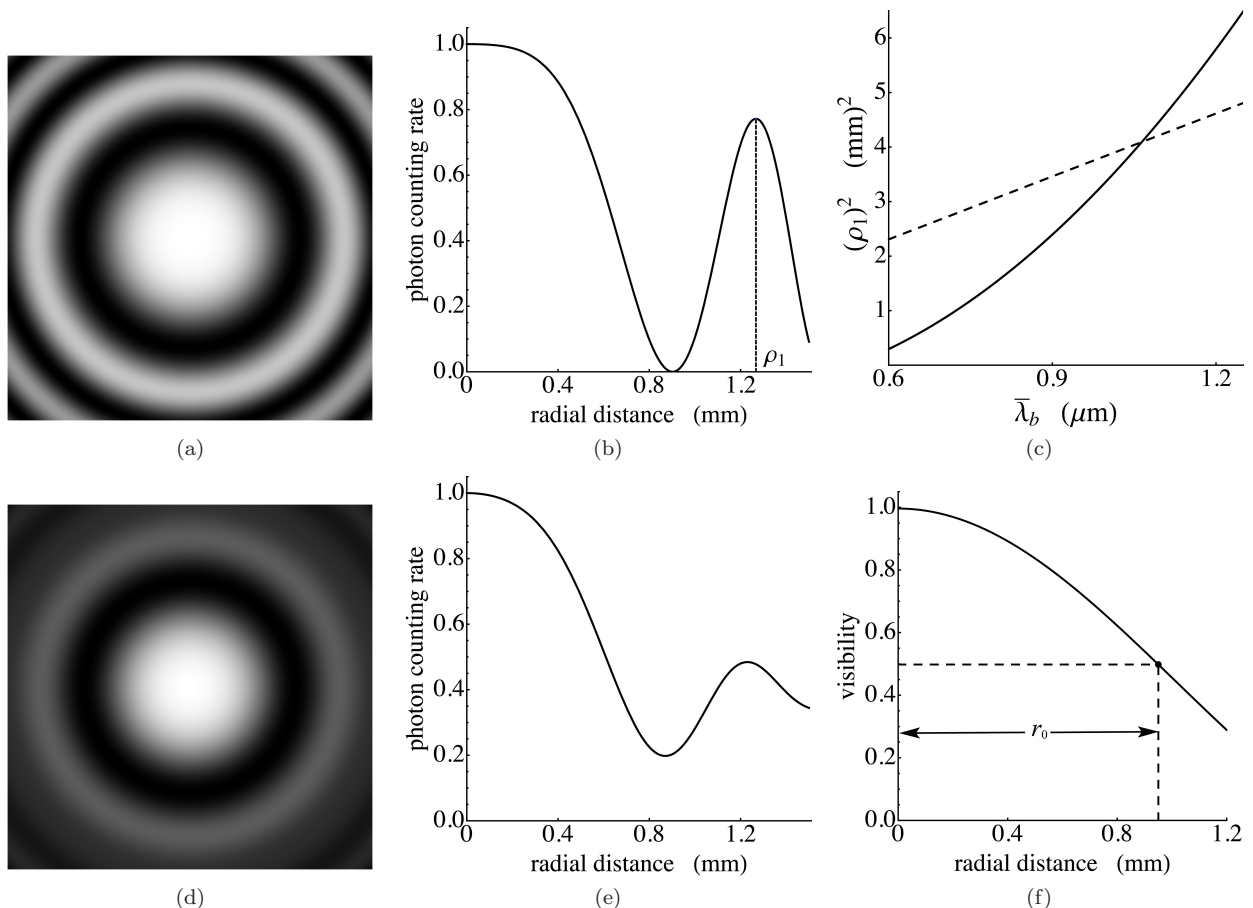


FIG. 4: Computationally obtained interference patterns when momenta of photons a and b are maximally correlated [(a), (b), (c)] and partially correlated [(d), (e), (f)]. Maximum correlation: (a) Circular fringes with maximum visibility shown on a $3 \text{ mm} \times 3 \text{ mm}$ screen for $d_a = 1.17 \text{ cm}$ and $\phi_0 = 0$. (b) Dependence of the normalized photon counting rate on $\rho_{k_b} \equiv |\rho_{k_b}|$ for the fringe pattern. The minimum value of the intensity is zero implying unit visibility. The radius of first ($N = 1$) bright ring (maximum) is ρ_1 . (c) Square of the radius, $(\rho_1)^2$, of the first bright ring plotted against the wavelength, λ_b , of the interfering light for our experiment (solid line) and for a Michelson interferometer (dashed line). Partial correlation: (d) Fringes of partial visibility shown on a $3 \text{ mm} \times 3 \text{ mm}$ screen for $d_a = 1.17 \text{ cm}$ and $\phi_0 = 0$. (e) Dependence of the normalized photon counting rate on ρ_{k_b} for the fringe pattern. Minimum value of the intensity is bigger than 0 implying less than unit visibility. (f) Visibility, $\mathcal{V}(\rho_{k_b})$, obtained by varying ϕ_0 at each point on the fringe pattern [shown in (d)] is plotted against the distance from the center of the pattern. The visibility at the center of the pattern: $\mathcal{V}(0) = 0.996$. The HWHM, r_0 , is the radial distance where the visibility drops to half of its value at $\rho_{k_b} = 0$.

while $\phi_b(\mathbf{k}_b)$ is fixed. The maximum (\mathcal{R}_{\max}) and minimum (\mathcal{R}_{\min}) values of the photon counting rate at each point are determined by varying ϕ_0 and the visibility is obtained by formula (9). We find that the visibility at each point is given by (see Appendix 2)

$$\mathcal{V}(\rho_{k_b}) = \frac{1}{\gamma} \exp(-\sigma_\theta^2 |\rho_{k_b}|^2 / \chi^2) \times |D_{-2}\{|\rho_{k_b}|g(\sigma_\theta)\} + D_{-2}\{-|\rho_{k_b}|g(\sigma_\theta)\}|, \quad (22)$$

where $A = \pi d_a \bar{\lambda}_a / (f_0 \bar{\lambda}_b)^2$, $B = f_0 \bar{\lambda}_b k'_0 / (2\pi)$, $\gamma = \sqrt{4 + \sigma_\theta^4 A^2 B^4}$, $\chi = \gamma / (AB)$, $g(\sigma_\theta) = i\sqrt{2}AB\sigma_\theta / \sqrt{2 - i\sigma_\theta^2 AB^2}$, and D_n is the parabolic cylinder function of order n . Figure 4(f) illustrates the dependence of the visibility on the distance from the center

of the pattern. The drop of visibility with the radial distance is characterized by the half width at half maximum (HWHM), i.e., by the distance, r_0 , from the center of the pattern, at which the visibility drops to the half of its value at the center.

Note that the maximum value of the visibility is obtained at $\rho_{k_b} = 0$, i.e., at the center of the fringe pattern. It follows from Eq. (22) that

$$\mathcal{V}(0) = \frac{2}{\gamma} = \frac{2}{\sqrt{4 + \sigma_\theta^4 A^2 B^4}}, \quad (23)$$

where we have used the fact $D_{-2}(0) = 1$. Clearly, when $\sigma_\theta \rightarrow 0$, i.e., when the momentum correlation is maximum, $\mathcal{V}(0) = 1$. In the other extreme case, when $\sigma_\theta \rightarrow \infty$, i.e., when the momentum correlation attains

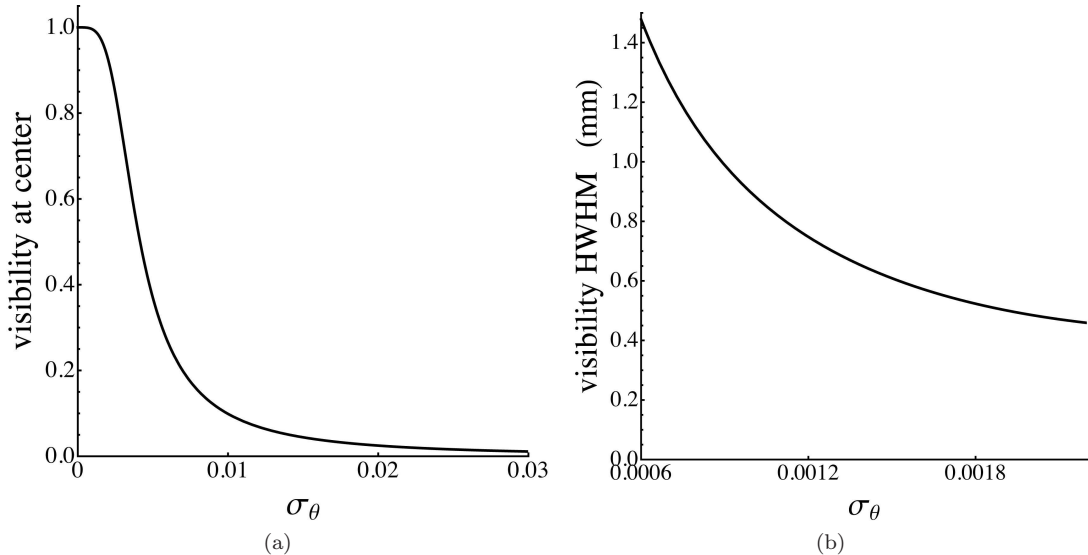


FIG. 5: Drop of visibility with decreasing momentum correlation, i.e., with increasing value of σ_θ . (a) Visibility at the center of the pattern [$\mathcal{V}(0)$] drops as σ_θ increases. (b) The HWHM, r_0 , [shown in Fig. 4(f)], is plotted against σ_θ . Higher value of σ_θ implies lesser momentum correlation and higher value of r_0 implies higher visibility. Chosen parameters: $d_a = 1.17$ cm, $\bar{\lambda}_a = 1550$ nm, $\bar{\lambda}_b = 810$ nm, and $\sigma_b = 1.67 \times 10^{-2}$.

the minimum value, $\mathcal{V}(0) = 0$. When σ_θ has a finite non-zero value, i.e., when the momenta of photons a and b are partially correlated, one has $0 < \mathcal{V}(0) < 1$. Figure 5(a) shows the dependence of $\mathcal{V}(0)$ on σ_θ . We further show, in Fig. 5(b), that the value of the visibility HWHM (r_0) decreases as σ_θ increases. Figures 5(a) and 5(b) thus clearly illustrate that the visibility of the pattern reduces as the transverse momenta of photons a and b becomes less correlated.

IV. DETERMINING THE MOMENTUM CORRELATION FROM THE FRINGE PATTERN

It is clear from the previous section that the correlation between the transverse momenta of photons a and b governs the visibility of the fringe pattern that is obtained by detecting photon b only. We now justify that under reasonable assumptions a quantitative measure of the momentum correlation between the two photons can be obtained from this visibility.

Let us first examine the example considered in Sec. III C. Using the expressions for A and B [see the text below Eq. (22)], one finds from Eq. (23) that

$$\sigma_\theta^2 = \frac{8\pi}{k_0'^2 \bar{\lambda}_a d_a} \left(\frac{1}{[\mathcal{V}(0)]^2} - 1 \right)^{\frac{1}{2}}. \quad (24)$$

It is thus clear that σ_θ can be uniquely determined from the visibility of the interference pattern. Since the conditional probability [see Eq. (21)] is given by $\mathcal{P}(\mathbf{k}_a|\mathbf{k}_b) \propto \exp[-2\theta'^2/\sigma_\theta^2]$, it can be immediately determined once σ_θ is known. (The conditional probability is often measured in the procedures that involve her-

alded detection [29, 30].) The quantity $P(\mathbf{k}_b)$ is directly obtained from the spatial dependence of the normalized photon counting rate in the camera when only one of the beams (b_1 or b_2) of photon b is detected. Now using Eq. (3), one can determine the joint probability $P(\mathbf{k}_a, \mathbf{k}_b)$ that governs the momentum correlation between the two photons a and b . Alternatively, the conditional probability can also be determined from the fact that the value of the visibility HWHM (r_0) reduces with decreasing momentum correlation (Fig. 5(b)).

We stress that the method of determining the joint probability (density) is not restricted to this particular example. If the two photons are not emitted into collinear or near-collinear beams, the momentum correlation can still be determined from the visibility of the fringes. In this case, however, the expression for visibility is no longer given by Eq. (22), and a more involved computational technique might be required to determine the conditional probability. The other assumptions made in our example are: 1) the photons are propagating in the form of paraxial beams; 2) $\mathcal{P}(\mathbf{k}_a|\mathbf{k}_b)$ is a function of $\mathbf{k}_a + \mathbf{k}_b$, i.e., of $\mathbf{p}_a + \mathbf{p}_b$; and 3) $\mathcal{P}(\mathbf{k}_a|\mathbf{k}_b)$ has a Gaussian form. Most traditional methods of determining momentum correlation usually require these three assumptions to be made. Note that our method applies to more general situations. When assumption 1 does not hold, the correlation between the longitudinal components of momenta also contributes to the visibility. However, a more involved detection system can in principle be employed to determine the correlation between the three-dimensional momenta of the two photons. Assumption 2 holds in many practical situations (see, for example, [31]). This assumption or an equivalent one might be necessary for

determining $\mathcal{P}(\mathbf{k}_a|\mathbf{k}_b)$. This is because Eq. (8) reduces to a three dimensional Fredholm integral equation of the first kind (in the continuous variable limit) only under such an assumption. This integral equation is uniquely solvable in principle; furthermore, in many cases its dimensionality can be reduced due to symmetries present in the system. It thus follows that a specific functional form of $\mathcal{P}(\mathbf{k}_a|\mathbf{k}_b)$ does not need to be assumed, i.e., assumption 3 is not essential.

V. COMPARISON WITH EXPERIMENTAL RESULTS

We have experimentally verified the above mentioned results [27, 28]. Here, we make a brief instructive comparison of our theoretical predictions with the experimental observations.

In the experiments, nonlinear crystals (ppKTP) pumped by mutually coherent laser beams have been used as biphoton sources. Each crystal can produce a photon pair (a , b) by the process of spontaneous parametric down-conversion. In this case, the wave vector, $\mathbf{k}' = \mathbf{k}_a + \mathbf{k}_b$, represents a wave vector of the pump.

The momentum correlation between the two photons is modulated by the tightness of focusing of the pump beam into the crystals. The tighter the focus of the pump, the bigger is the range over which \mathbf{k}' can vary for a particular choice of \mathbf{k}_b , i.e., the value of σ_θ increases (see Eq. (21)). For a Gaussian pump waist w_p , one has $\sigma_\theta = \bar{\lambda}_p/(\pi w_p)$, where $\bar{\lambda}_p = 2\pi/k'_0$ is the mean wavelength of the pump beam (see endnote [25]). The experimental values of $\bar{\lambda}_p$, $\bar{\lambda}_a$, and $\bar{\lambda}_b$ are 532 nm, 1550 nm, and 810 nm, respectively.

To achieve a high quality alignment of the beams of photon a , a $4f$ lens system was placed between the two sources (crystals) on the path of the a -photon beam. When the $4f$ lens system is fully balanced, it images the first source (Q_1) on the second source (Q_2). In this case, the effective propagation distance, d_a , between the two sources becomes zero. Nonzero values of d_a were obtained by unbalancing the $4f$ lens system (for further details see [27]).

Figure 6 shows fringe patterns obtained for different values of d_a , when the pump is highly collimated (very weakly focused at the crystals). The consequent high momentum correlation between photons a and b results in fringes with high visibility as suggested by the theoretical analysis. The equivalent wavelength, $\bar{\lambda}_{eq}$, has been determined experimentally and found to be 420 ± 7 nm, where the theoretically predicted value is approximately 423 nm.

Figure 7 shows that the fringes blur out as the pump beams are more tightly focused at the crystals. It illustrates that when the momentum correlation between the two photons reduces, the visibility also reduces. In the experiment, the dependence of the visibility on the distance from the center of the pattern was measured for

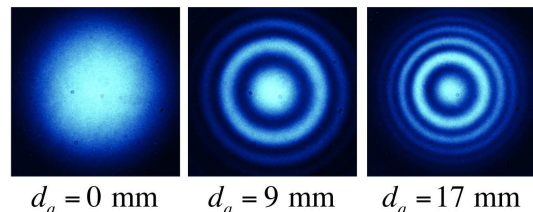


FIG. 6: (Adapted from [27].) Experimentally observed fringes for different values of the effective propagation distance (d_a), when the pump beams were highly collimated. The equivalent wavelength, $\bar{\lambda}_{eq}$, which characterizes the fringe shift associated with d_a was experimentally determined and found to be 420 ± 7 nm; the theoretically predicted value is 423 nm. One does not need to know the wavelengths of the pump, a , and b photons for the experimental determination of $\bar{\lambda}_{eq}$.

different values of w_p . It was found that the visibility

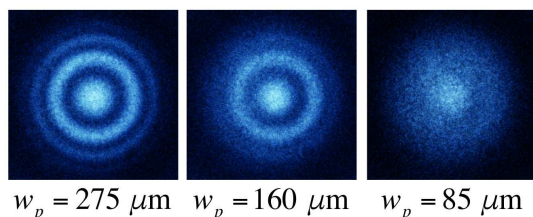


FIG. 7: (Adapted from [28].) Experimentally observed fringes for different values of the pump waist at the crystals and a fixed value of $d_a = 11.7$ mm. The values of σ_θ corresponding to the pump waists (left to right) are 6.16×10^{-4} , 1.06×10^{-3} , and 1.99×10^{-3} , respectively. The fringe visibility drops as the momentum correlation between the two photons reduces.

drops with the radial distance as suggested by Fig. 4(f). The experimentally obtained dependence ([28], Fig. 2B) of the corresponding FWHM ($2r_0$) on w_p matches with the theoretical dependence predicted by Eq. (22). The variance of the conditional transverse momentum correlation was also determined from the visibility of the fringes; for further details see [28].

VI. SUMMARY AND CONCLUSION

We have shown that by using two spatially separated identical biphoton sources a novel single-photon fringe pattern can be created. We have restricted the analysis to circular fringes that resemble fringes of equal inclination ([19], Sec. 7.5.1). It is not difficult to envision that fringes of equal thickness ([19], Sec. 7.5.2) can also be created in our system: this can be done by a slight misalignment of the beams a_1 and a_2 when the distance between the sources is very small. Our system can therefore produce interference fringes that resemble the fringes observed in a Michelson interferometer ([19], Sec. 7.5.4). However, in contrast to our system, a Michelson interferometer superposes two beams that are created from a

single beam by division of amplitude. In our case, the interfering beams are generated separately by two sources that produce photon pairs. Furthermore, the interference fringes produced in our system have some novel properties. These fringes are obtained by detecting only one photon of each photon pair. We have discussed in Sec. III A that the fringes shift when the optical path traversed by the undetected photon changes. This fringe shift is characterized by a combination of wavelengths of both photons, which we experimentally demonstrate in Ref. [27]. This phenomenon allows us to determine the wavelength of a photon without detecting it.

A striking feature of the fringe pattern is that the visibility decreases with decreasing correlation between the transverse momenta of each photon pair. This observation opens up a new avenue for measuring correlation between two quantum entities. As shown in Sec. IV, this property of the fringes can be used to determine the momentum correlation. The result is remarkable because most traditional methods of measuring any sort of correlation between photons of a pair involve coincidence or an equivalent detection technique (see, for example, [29, 30, 32–37]). In our method, no coincidence or heralded detection or post selection is required [38]; only measuring the single-photon counting rate is enough. Since we do not need to detect one of the photons of the pair, the method allows us to access wavelengths for which good detectors are not available. This fact also extends the experimental reach.

Measurement of the correlation between transverse momenta of two photons is essential for the verification of spatial entanglement. Furthermore, we believe that our method can be generalized to measure position correlation between two photons and also to other degrees of freedom (for example, one can apply it to measure spectral correlation of biphotons). Our results therefore open up the possibility of developing a novel method of verifying entanglement without coincidence or heralded detection [39]. Since entanglement plays a vital role in fundamental tests of quantum mechanics [40–43] and has important applications in quantum information and communication science (see, for example, [44]), we expect that this direction of research will have a broad significance in the future.

Finally, recent experimental developments in the fields of microwave superconducting cavities [18], trapped ions [45], atomic systems [46, 47], and superconducting circuits [48] shows the possibility of generalizing our method to other quantum mechanical entities.

Acknowledgments

We thank Dr. Fabian Steinlechner for useful discussions. This work was supported by the Austrian Academy of Sciences (ÖAW- IQOQI, Vienna), and the Austrian Science Fund (FWF) with SFB F40 (FOQUS) and W1210-2 (CoQus). R.L. was supported by National

Science Centre (Poland) grants 2015/17/D/ST2/03471, 2015/16/S/ST2/00424, the Polish Ministry of Science and Higher Education, and the Foundation for Polish Science (FNP).

Appendix 1

We show the derivation of Eq. (4).

It follows from Eq. (1) that the by photon state generated by each source can be represented as

$$\begin{aligned} |\psi_j\rangle &= \sum_{\mathbf{k}_{a_j}, \mathbf{k}_{b_j}} C_{\mathbf{k}_a, \mathbf{k}_b} |\mathbf{k}_{a_j}\rangle_{a_j} |\mathbf{k}_{b_j}\rangle_{b_j} \\ &= \sum_{\mathbf{k}_a, \mathbf{k}_b} \left[C_{\mathbf{k}_{a_j}, \mathbf{k}_{b_j}} \hat{a}_{a_j}^\dagger(\mathbf{k}_{a_j}) \hat{a}_{b_j}^\dagger(\mathbf{k}_{b_j}) + \text{h.c.} \right] |0\rangle_{a_j} |0\rangle_{b_j}, \end{aligned} \quad (25)$$

where $j = 1, 2$ label the sources, $|0\rangle$ represents a vacuum state, and \hat{a}_a^\dagger and \hat{a}_b^\dagger represents creation operators of photons a and b , respectively, and h.c. represents Hermitian conjugate. When beam a_1 is sent through source Q_2 and is aligned with beam a_2 , one has for each mode \mathbf{k}_a

$$\hat{a}_{a_2}(\mathbf{k}_a) = \exp[i\phi_a(\mathbf{k}_a)] \hat{a}_{a_1}(\mathbf{k}_a), \quad (26)$$

where $\phi_a(\mathbf{k}_a)$ is the phase acquired by the plane-wave mode \mathbf{k}_a due to propagation from Q_1 to Q_2 .

Since photon pairs emitted by both sources are never simultaneously present in our system, the quantum state of light is obtained by a linear superposition of the states generated by each source with the condition imposed by Eq. (26). Equation (4) thus immediately follows from Eqs. (25) and (26).

Appendix 2

We discuss some mathematical steps used in Sec. III C following Eq. (20).

Recall that θ' , θ_a , and θ_b are the angles made by \mathbf{k}' , \mathbf{k}_a , and \mathbf{k}_b , respectively, with the optical axis; θ' , θ_a , and θ_b are very small angles. Using the fact that the change in ϕ_a is due to change in propagation distance d_a , ϕ_a is expressed in terms of d_a and θ_a as shown in Eq. (12) of Sec. III A; θ_a is further expressed in terms of θ' and θ_b using the condition $\mathbf{k}' = \mathbf{k}_a + \mathbf{k}_b$. Substituting for ϕ_a into Eq. (20), using the assumed forms of $P(\mathbf{k}_b)$ and $|\mu(\mathbf{k}')|$, and replacing the summation by an integration, we obtain

$$\begin{aligned} \mathcal{R}(\boldsymbol{\rho}_{\mathbf{k}_b}) &\propto \int_0^{\Delta\theta} d\theta' \exp(-2\theta'^2/\sigma_\theta^2) \exp[-2|\boldsymbol{\rho}_{\mathbf{k}_b}|^2/(f_0\sigma_b)^2] \\ &\quad \times \theta' \{ 2 + \cos[A(B\theta' - |\boldsymbol{\rho}_{\mathbf{k}_b}|)^2 - \phi_0] \\ &\quad + \cos[A(B\theta' + |\boldsymbol{\rho}_{\mathbf{k}_b}|)^2 - \phi_0] \}, \end{aligned} \quad (27)$$

where $A = \pi d_a \bar{\lambda}_a / (f_0 \bar{\lambda}_b)^2$, $B = f_0 \bar{\lambda}_b k'_0 / (2\pi)$, $\Delta\theta$ is the maximum range up to which θ' can vary ($\sigma_\theta \ll \Delta\theta$), and

we have used the relations $P(\mathbf{k}_b) = \exp[-2\theta_b^2/\sigma_b^2]$ and $|\boldsymbol{\rho}_{\mathbf{k}_b}|^2 \approx f_0^2\theta_b^2$. Since $\sigma_\theta \ll \Delta\theta$, the upper limit of the integration in Eq. (27) can be replaced by ∞ , and the integral can be expressed in terms of standard integrals whose values are known [49]. An explicit form of $\mathcal{R}(\boldsymbol{\rho}_{\mathbf{k}_b})$ can thus be obtained and is found to have the form

$$\mathcal{R}(\boldsymbol{\rho}_{\mathbf{k}_b}) \propto 1 + \mathcal{V}(\boldsymbol{\rho}_{\mathbf{k}_b}) \cos[\phi_0 + \beta(\boldsymbol{\rho}_{\mathbf{k}_b})], \quad (28)$$

where $\mathcal{V}(\boldsymbol{\rho}_{\mathbf{k}_b})$ is given by Eq. (22); an explicit form of $\beta(\boldsymbol{\rho}_{\mathbf{k}_b})$ is not required for determining the visibility.

-
- [1] A. A. Michelson, “The relative motion of the earth and the luminiferous ether,” *Am. J. Sci.* **22**, 120-129 (1881).
- [2] A. A. Michelson and E. Morley, “On the relative motion of the earth and the luminiferous ether,” *Am. J. Science* **34**, 333-345 (1887).
- [3] A. Einstein, “Zur Elektrodynamik bewegter Körper,” *Ann. d. Phys.* **17**, 891-921 (1905).
- [4] A. D. Cronin, J. Schmiedmayer, and D. E. Pritchard, “Optics and interferometry with atoms and molecules,” *Rev. Mod. Phys.* **81**, 1051-1129 (2009).
- [5] B. P. Abbott et al., “Observation of gravitational waves from a binary black hole merger,” *Phys. Rev. Lett.* **116**, 061102 (2016).
- [6] X. Y. Zou, L. J. Wang and L. Mandel, “Induced Coherence and Indistinguishability in Optical Interference,” *Phys. Rev. Lett.* **67**, 318-321 (1991).
- [7] L. J. Wang, X. Y. Zou and L. Mandel, “Induced Coherence without Induced Emission,” *Phys. Rev. A* **44**, 4614-4622 (1991).
- [8] R. P. Feynman, R. B. Leighton and M. Sands, *The Feynman Lectures on Physics, Vol. III*, (Addison-Wesley Publishing Company, New York, USA 1966).
- [9] G. B. Lemos, V. Borish, G. D. Cole, S. Ramelow, R. Lapkiewicz and A. Zeilinger, “Quantum imaging with undetected photons,” *Nature* **512**, 409-412 (2014).
- [10] M. Lahiri, R. Lapkiewicz, G. B. Lemos and A. Zeilinger, “Theory of quantum imaging with undetected photons,” *Phys. Rev. A* **92**, 013832 (2015).
- [11] S. P. Kulik, G. A. Maslennikov, S. P. Merkulova, A. N. Penin, L. K. Radchenko, and V. N. Krasheninnikov, “Two-photon interference in the presence of absorption,” *J. Exp. Theor. Phys.* **98**, 3138 (2004).
- [12] D. A. Kalashnikov, A. V. Paterova, S. P. Kulik, and L. A. Krivitsky, “Infrared spectroscopy with visible light,” *Nat. Phot.* **10**, 98-101 (2016).
- [13] M. Lahiri, A. Hochrainer, R. Lapkiewicz, G. B. Lemos, and A. Zeilinger, “Partial Polarization by Quantum Distinguishability,” Submitted (arXiv:1510.04192).
- [14] T. J. Herzog, J. G. Rarity, H. Weinfurter, and A. Zeilinger, “Frustrated two-photon creation via interference,” *Phys. Rev. Lett.* **72**, 629-632 (1994).
- [15] T. J. Herzog, P. G. Kwiat, H. Weinfurter, and A. Zeilinger, “Complementarity and the Quantum Eraser,” *Phys. Rev. Lett.* **75**, 3034-3037 (1995).
- [16] A. Heuer, R. Menzel, and P. W. Milonni, “Induced Coherence, Vacuum Fields, and Complementarity in Biphoton Generation,” *Phys. Rev. Lett.* **114**, 053601 (2015).
- [17] A. Heuer, R. Menzel, and P. W. Milonni, “Complementarity in biphoton generation with stimulated or induced coherence,” *Phys. Rev. A* **92**, 033834 (2015).
- [18] P. Lähteenmäki, G. S. Paraoanu, J. Hassel, and P. J. Hakonen, “Coherence and multimode correlations from vacuum fluctuations in a microwave superconducting cavity,” *Nat. Commun.* **7**, 12548 (2016).
- [19] M. Born and E. Wolf, *Principles of Optics* (Cambridge University Press, Cambridge, 7th Ed. 1999).
- [20] The idea of aligning the two beams was originally suggested by Z. Y. Ou [6].
- [21] Since \mathbf{k}_a and \mathbf{k}_b are continuous variables, the summation is to be interpreted as an integration. We use the summation symbol for simplicity.
- [22] R. J. Glauber, “The quantum theory of optical coherence” *Phys. Rev.* **130**, 2529 (1963).
- [23] In case the propagation length cannot be changed appreciably due to experimental constraints, a similar phase change can be introduced by using an appropriate lens system or phase shifters.
- [24] This situation occurs when the photon pair is produced by collinear or near-collinear down-conversion process. In such a case one needs to consider the effect of refraction at the crystal surface. This, however, does not change any of our results.
- [25] When the photon pair is produced by spontaneous parametric down-conversion, $k'_0 = 2\pi/\lambda_p$, where λ_p is the mean wavelength of the pump photon.
- [26] The delta function has been used to approximately represent the very narrow frequency bandwidth of the pump photon. The Gaussian dependence on θ' has been observed experimentally in several cases (see, for example, [29, 30]).
- [27] A. Hochrainer, M. Lahiri, G. B. Lemos, R. Lapkiewicz and A. Zeilinger, “Interference Fringes Controlled by Non-Interfering Photons,” *Optica* **4**, 341-344 (2017).
- [28] A. Hochrainer, M. Lahiri, G. B. Lemos, R. Lapkiewicz and A. Zeilinger, “Quantifying the momentum correlation between two light beams by detecting one,” *Proc. Nat. Acad. Sci. USA* **114**, 1508-1511 (2017).
- [29] J. C. Howell, R. S. Bennink, S. J. Bentley, and R. W. Boyd, “Realization of the Einstein-Podolsky-Rosen paradox using momentum- and position-entangled photons from spontaneous parametric down conversion,” *Phys. Rev. Lett.* **92**, 210403 (2004).
- [30] M. P. Edgar, D. S. Tasca, F. Izdebski, R. E. Warburton, J. Leach, M. Agnew, G. S. Buller, R. W. Boyd, and M. J. Padgett, “Imaging high-dimensional spatial entanglement with a camera,” *Nat. Commun.* **3**, 984 (2012).
- [31] D. S. Tasca, S. P. Walborn, P. H. Souto Ribeiro, F. Toscano, and P. Pellat-Finiet, “Propagation of transverse intensity correlations of a two-photon state,” *Phys. Rev. A* **79**, 033801 (2009).
- [32] H. Di Lorenzo Pires, C. H. Monken, and M. P. van Exter, “Direct measurement of transverse-mode entanglement

- in two-photon states,” *Phys. Rev. A* **80**, 022307 (2009).
- [33] K. Laiho, A. Christ, K. N. Cassemiro, and C. Silberhorn, “Testing spectral filters as Gaussian quantum optical channels,” *Opt. Lett.* **36**, 1476-1478 (2011).
- [34] G. A. Howland and J. C. Howell, “Efficient high-dimensional entanglement imaging with a compressive-sensing double-pixel camera,” *Phys. Rev. X* **3**, 011013 (2013).
- [35] F. Just, A. Cavanna, M. V. Chekhova, and G. Leuchs, “Transverse entanglement of biphotons,” *New J. Phys.* **15**, 083015 (2013).
- [36] D. S. Tasca, Lukasz Rudnicki, R. M. Gomes, F. Toscano, and S. P. Walborn, “Reliable Entanglement Detection under Coarse-Grained Measurements,” *Phys. Rev. Lett.* **110**, 210502 (2013).
- [37] M. Hor-Meyll, J. O. de Almeida, G. B. Lemos, P. H. Souto Ribeiro, and S. P. Walborn, “Ancilla-Assisted measurement of photonic spatial correlations and entanglement,” *Phys. Rev. Lett.* **112**, 053602 (2014).
- [38] Theoretical calculations on probing multimode squeezing with correlation functions [50] show that it would also be possible to determine correlation between two photons from the intensity correlation measured by detecting only one of them. A followup experiment ([33], Fig. 2(b)) verified the conclusion, albeit the other photon was also detected and eventually the “heralded” intensity correlation was measured.
- [39] Under the assumption that the photon pair is in a pure state, measurement of the lowest-order spatial coherence in one beam has been used to verify spatial entanglement of the pair (see, for example, [35]).
- [40] A. Einstein, B. Podolsky, and N. Rosen, “Can quantum-mechanical description of physical reality be considered complete?” *Phys. Rev.* **47**, 777-780 (1935).
- [41] D. Bohm, “A suggested interpretation of the quantum theory in terms of “hidden” variables. I,” *Phys. Rev.* **85**, 166-179 (1952).
- [42] D. Bohm, “A suggested interpretation of the quantum theory in terms of “hidden” variables. II,” *Phys. Rev.* **85**, 180-193 (1952).
- [43] J. S. Bell, “On the Einstein Podolsky Rosen paradox” *Physics* **1**, 195-200 (1964).
- [44] R. Horodecki, P. Horodecki, M. Horodecki, and K. Horodecki, “Quantum entanglement,” *Rev. Mod. Phys.* **81**, 865-942 (2009).
- [45] R. Blatt and D. Wineland, “Entangled states of trapped atomic ions,” *Nature* **453**, 1008-1015 (2008).
- [46] M. Keller, M. Kotyrba, F. Leupold, M. Singh, M. Ebner, and A. Zeilinger, “Bose-einstein condensate of metastable helium for quantum correlation experiments,” *Phys. Rev. A* **90**, 063607 (2014).
- [47] R. Lopes, A. Imanaliev, A. Aspect, M. Cheneau, D. Biron, and C. I. Westbrook, “Atomic Hong-Ou-Mandel experiment,” *Nature* **520**, 66-68 (2015).
- [48] R Barends, et al., “Superconducting quantum circuits at the surface code threshold for fault tolerance,” *Nature* **508**, 500-503 (2014).
- [49] I.S. Gradshteyn and I.M. Ryzhik, *Table of Integrals, Series, and Products* (Academic Press, New York, 7th Ed. 2007); Eqs. 3.461(3) and 3.462(1).
- [50] A. Christ, K. Laiho, A. Eckstein, K. N. Cassemiro, and C. Silberhorn, “Probing multimode squeezing with correlation functions,” *New J. Phys.* **13**, 033027 (2011).